Bayer *et al.*[11] and Korkusinski *et al.*[14] formulated simple models for the energies of the four excitons starting from Eq. (2) in a double dot and compared the predicted energies with experiment. Experimentally, the emission spectra of a dot molecule showed[11,14] two exciton transitions separated by an energy ΔE. This energy ΔE was shown to increase with decreasing interdot separation. This observation was in agreement with the theory where the same behavior was obtained.

two bright states

stance, be modeled by simple single-band effective-mass models. Furthermore, the assumption $t_e = t_h$

starting from $In_{0.5}Ga_{0.5}As$ at the base, to pure InAs at the top of the dots. Both dots have one monolayer wetting layer. The

III. RESULTS FOR THE SINGLE-PARTICLE STATES

A. Largely separated dots ($d \to \infty$)

Figure 1(b) shows the single-particle electron and hole energies as a function of interdot separation. For large interdot separations the single-particle hole states h_0 and h_1 are energetically almost degenerate. Figures 4 and 5 show the electron and hole wave functions as a function of the interdot separation d. In these figures, the envelope functions f_n [see Eq. (13)] averaged over eight atom cells are plotted. The physical shape of the dot (truncated cones) is shown in grey, whereas the wave functions are depicted as two isosurfaces with two shades of color enclosing 75% and 40% of the state density. The hole states h_0 and h_1 are localized on the bottom and top dots, respectively (Fig. 5). This behavior resembles H_2^+ with very long bond length where the orbitals are local-

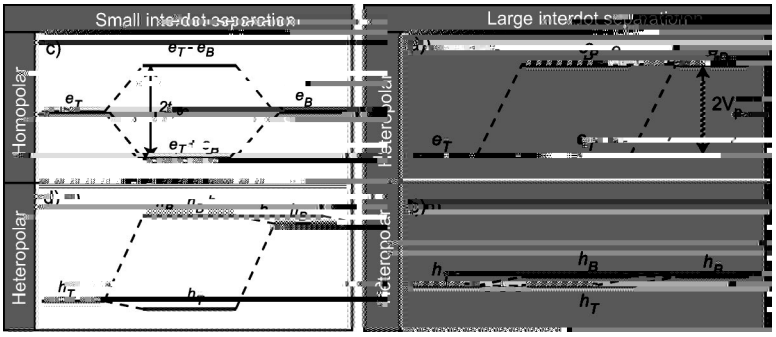

FIG. 6. Formation of single-particle "molecular orbitals" (MO's) [in the central part of panels (a), (b), (c), (d)] from the single-particle "atomic orbitals" [on the left and right sides of panels (a), (b), (c), (d)]. For large interdot separation the electrons and the hole form heteronuclearlike MO's. For small separation the electrons form bonding-antibonding combinations like homonuclear MO's.

symmetry-broken (heteronuclearlike) states. Figures 6(c) and 6(d) show this hybrid behavior where electrons form symmetric-antisymmetric combinations of MO's, akin to a homonuclear dimer, while holes give rise to heteronuclear MO's localized on one or the other dot. There are two reasons for this behavior, explained in the following two paragraphs.

1. Hole states experience a high barrier that suppresses interdot tunneling

The first reason for the broken-symmetry hole behavior is the high barrier between the two dots experienced by the heavy-hole component (dominant) of the hole states. To appreciate these facts we performed strained modified band offsets calculations (Sec. II C) for different interdot separations. Figure 7 shows the results for the first two hole confining potentials for three different interdot separations. The character [heavy hole, $J(xy)$, and $J(z)$] of each eigenstate is represented by a certain symbol of size proportional to the weight of the character. The heavy-hole confining potential is the relevant quantity for the energetics of the hole states since hole states are to over 80% heavy hole like. Examination of the heavy-hole confining potential (circles in Fig. 7) reveals that the potential is *negative* in the region of the barrier, strongly repelling heavy holes. This high barrier was also reported[28] for pure InAs truncated-pyramid dots. Furthermore, the effective barrier felt by the hole states increases upon reduction of the interdot separation, suppressing tunneling and the ability for holes to form bonding-antibonding states. Figure 1(b) also shows that the hole states move to lower energy when the interdot separation is reduced, in agreement with the increasing barrier height between the dots.

2. Due to the lack of inversion symmetry between the dots, the bottom dot is more favorable for holes

The lack of inversion symmetry between nonspherical (e.g., lens-shaped) dots leads to heteronuclear hole states. This can be seen in the top panel of Fig. 7 where indeed the confinement potential experienced at the base of the *top* dot is different than that experienced at the base of the *bottom* dot. Figure 1(b) shows that the hole states h_0 and h_1, which are energetically almost degenerate at large interdot separation, split when the distance is reduced, showing an increasing preference for holes to be in the bottom dot with diminishing interdot separation. This can be understood using a simple strain picture like given in Fig. 8. A single truncated-cone or truncated-pyramid dot with homogeneous composition is nearly unstrained on the apex while it is stained at the base. The top right panels of Fig. 8 show a cubical unit cell for the unstrained case and an elongated parallelepiped for the case of biaxial strain. The heavy holes prefer the highly strained region near the base and localize preferentially in

FIG. 7. Strain-modified confining potential for holes along the growth direction (001) (given in the inset of the top panel) for three dot molecules with a base-to-base separations of 5.1, 11.3, and 22.6 nm. Each data point is an average over the results obtained in the the (001) plane. The size of the circles is proportional to the weight of the heavy-hole contributions; the sizes of the triangles pointing upward [downward] are proportional to the weight of the $J(xy)$ [$J(z)$] contributions.

this region as suggested by the strained bulk band structure given on the right side of Fig. 8. When two dots are close together the strain at the top but also at the base of the upper dot is almost hydrostatic due to the compression of the dot through the sandwiched material. The base of the lower dot, however, experiences biaxial strain and remains favorable for heavy holes. The magnitude of this effect should be stronger for pure InAs dots since it experiences more strain than our alloyed InGaAs dot. With a very strong preference for hole states to localize on the bottom dot, not only the first (like on our case), but the first few hole states might localized on the bottom dot. This expected behavior has been reported by Sheng and Leburton[28] performing eight band $\mathbf{k}\cdot\mathbf{p}$ calculations of a pure InAs truncated-pyramid dot molecule where the first two single-particle hole states are localized on the bottom dot. Such a localization might have detrimental consequences for the achievement of entanglement.

3. Component of the hole wave function responsible for the hole tunneling has P symmetry

Figure 7 shows how the $J(z)$ confinement potential (triangles pointing downwards) becomes attractive between the dots at small interdot separation. The effect of this attractive potential on the hole state h_0 is shown in Fig. 9, where the single-particle hole state h_0 of our pseudopotential calculation is decomposed according to its Bloch—and envelope function—character [see Eq. (17)]. Only the main contributions—the symmetric heavy-hole state with pure S envelope function and the antisymmetric $J(z)$ state with pure P envelope function—are shown. Figure 9 shows that when the interdot distance is reduced, the heavy-hole character diminishes while the $J(z)$ character increases. This is in agreement with the qualitative picture given by the strained-modified band-offset calculation where the $J(z)$ confining potential becomes attractive between the dots at small interdot separation. The part of the (multiband) wave function responsible for the hole tunneling is therefore antisymmetric P

A. Largely separated dots

energies [Fig. 1(b)]. This destabilization goes along with delocalization of these states. With decreasing interdot distance, the single-particle electron state e_0 becomes delocalized as well, but for another reason: it creates a bonding state with increased occupation probability between the dots (Fig. 4). Both the delocalization of the electron state e_0 and the delocalization of the hole states h_0 and h_1 contribute to lower the *e*-*h* Coulomb attractions U_{eh}^{TT} and U_{eh}^{BB}. The delocalization of the excited hole state h_1 (localized on top) is stronger than the delocalization of h_0. The magnitude of U_{eh}^{TT} is therefore reduced more severely than U_{eh}^{BB} with decreasing d. This shift is an excitonic effect which is missed by theories restricted to the single-particle level.[28,32]

C. Anticrossing of $|1\rangle$ and $|2\rangle$ at d_c: Bonding-antibonding exciton splitting

At the critical distance d_c the energy difference between $|1\rangle \simeq |e_T h_T\rangle$ and $|2\rangle \simeq |e_B h_B\rangle$ is very small, allowing them to form bonding and antibonding excitons $|e_T h_T\rangle + |e_B h_B\rangle$ and $|e_T h_T\rangle - |e_B h_B\rangle$ as shown in the "critical d" column of Fig. 3. The energy difference between these excitons is 0.4 meV and is conceptionally very similar to the Davydov splitting[33] observed in molecular crystals. Since the excitons $|e_T h_T\rangle$ and $|e_B h_B\rangle$ are highly symmetric, their bonding and antibonding combinations should yield highly symmetric and antisymmetric excitons with strong entanglement. A quantitative analysis of the entanglement will be given subsequently. Interestingly the antibonding combination (optically dark) is energetically below the bonding combination (optically bright). This is due to the fact that the single-particle hole states do not form an *ss*

our results. Earlier, Migliorato *et al.*[39] reported a redshift of the ensemble PL for stacks of vertically aligned quantum dots. Our predicted blueshift only applies to quantum dots separated by enough buffer material to still be distinct entities. The limiting case of a base-to-base separation equal to the dot height naturally yields a redshift typical of the formation of one single larger quantum dot. The theoretical results for the magnitude of the splitting of the bright states $|2\rangle$ and $|3\rangle$ in Fig. 2(c) are in good agreement with the experiments.[11–14] The agreement is even better if a systematic error of 1 nm between the interdot separation given in the experiments and the calculated base-to-base separation is assumed. We then compare the theoretical results: 42.1, 32.8, 24.8, and 16.8 meV (for the separations 5.1, 5.7, 6.8, and11–14

the detailed results of the pseudopotential-CI calculations and the derived tight-binding picture, possible to derive.

VI. SUMMARY

We have shown that the proper theoretical treatment of excitons in dot molecules requires an accurate description on the single-particle level (multiband coupling and strain effects must be taken into account; single-band approaches miss the qualitative picture) as well as on the few-particle level. We showed that simplified high-symmetry models commonly used in the literature yield qualitatively erroneous results.

At short interdot separations, the single-particle physics of the electron states is close to the one of a homonuclear dimer where the orbitals form bonding and antibonding states. The hole states remain, even at short interdot distance, localized on one or the other dot. We showed that the hole behavior can be explained by (i) strain, which inhibits the tunneling, and (ii) the lack of inversion symmetry between self-assembled quantum dots. This hybrid homo-nuclear-heteronuclear behavior of electrons and holes leads to four optically allowed excitons with low degree of entanglement.

At large interdot separation, both the electron and hole behave like a heteronuclear molecule forming two bright and two dark excitonic states, all four unentangled.

At a critical distance of 8.5 nm